Semiclassical relation between open trajectories and periodic orbits for the Wigner time delay

Jack Kuipers* and Martin Sieber†
School of Mathematics, University of Bristol, Bristol BS8 1TW, United Kingdom
(Received 6 December 2007; published 25 April 2008)

The Wigner time delay of a classically chaotic quantum system can be expressed semiclassically either in terms of pairs of scattering trajectories that enter and leave the system or in terms of the periodic orbits trapped inside the system. We show how these two pictures are related on the semiclassical level. We start from the semiclassical formula with the scattering trajectories and derive from it all terms in the periodic orbit formula for the time delay. The main ingredient in this calculation are correlations between scattering trajectories which are due to trajectories that approach the trapped periodic orbits closely. The equivalence between the two pictures is also demonstrated by considering correlation functions of the time delay. A corresponding calculation for the conductance gives no periodic orbit contributions in leading order.

DOI: 10.1103/PhysRevE.77.046219 PACS number(s): 05.45.Mt, 03.65.Sq

I. INTRODUCTION

Quantum systems whose classical counterparts are chaotic show universal statistical fluctuations that are well modeled by random matrix theory (RMT) [1,2]. In the semiclassical limit, formally as $\hbar \to 0$, the quantum statistics can be approximated by quantities that involve trajectories of the classical dynamics. One focus of work in semiclassics has been to recreate results from RMT by semiclassical methods.

For closed systems, statistical fluctuations in the energy spectrum can be seen, for example, in the spectral form factor $K(\tau)$ which is semiclassically approximated by a double sum over periodic orbits. The universal fluctuations from RMT are then due to correlated pairs of periodic orbits. The diagonal approximation, comparing an orbit to itself (or its time reverse) leads to the first term in the expansion of the form factor [3,4]. All the other terms in the small time ($\tau < 1$) expansion of the form factor can be obtained, in agreement with RMT, from periodic orbits with self-encounters. These are events where an orbit approaches itself (or its time reverse) very closely so that its partner can cross the encounter region differently [5,6]. Currently it is not known what other type of periodic orbit correlations contribute in the regime $\tau > 1$, though their contribution is calculated indirectly in Refs. [7,8]. Similar methods as for the form factor have been applied, for example, to the conductance through open systems where the semiclassical sum is over pairs of open trajectories that start and end in the leads [9–11].

For the Wigner time delay in open systems we have the interesting situation that the semiclassical approximation can be expressed in two ways. One gives the time delay as a double sum over scattering trajectories that enter and leave the system, in a similar way as for the conductance. The other is through a relation to a density of states and leads to a semiclassical formula that contains the average time delay plus a single sum over the periodic orbits that are trapped in the system. Our main motivation for this article is to understand the duality of these two semiclassical pictures. For open chaotic cavities, we will start from one of these pictures, the double sum over scattering trajectories, and derive all terms in the other semiclassical formula for the time delay. The periodic orbit terms are obtained by considering open trajectory correlations which are linked to the motion around periodic orbits. For systems without time-reversal symmetry these periodic orbit encounters are sufficient for obtaining the correct periodic orbit terms. For systems with time-reversal symmetry one also has to include combinations of self-encounters and periodic orbit encounters. Trajectories which approach periodic orbits play also a role in conductance fluctuations and have been considered in Ref. [12].

We will also consider a correlation function of the time delay. When expressed as a double sum over periodic orbits, the diagonal approximation [13,14] and higher order terms [15] were shown to agree with RMT (for a small time expansion). Using the other semiclassical approximation which is in terms of a quadruple sum over open trajectories, it was shown in Ref. [16] that the diagonal approximation does not give the leading RMT result. This was attributed to the nonunitarity of the semiclassical scattering matrix [17]. The inclusion of off-diagonal terms due to trajectories with self-encounters removes the discrepancy with RMT and restores the semiclassical unitarity of the scattering matrix. A brief account of this was given in Ref. [18]. These calculations are similar to those for correlation functions of the conductance [19,12,11].

Our paper is divided as follows. In Sec. II we introduce the two semiclassical approaches for the time delay. In Sec. III we show which correlated pairs of open trajectories recreate the average time delay. We then go beyond the average to recreate the periodic orbit contributions in Sec. IV. This is achieved by introducing the new type of trajectory correlations which are due to periodic orbit encounters. The correlation function of the time delay is considered in Sec. V, and our conclusions follow in Sec. VI.

II. THE TIME DELAY

For a chaotic cavity with one or more open leads that carry M scattering channels, the incoming and outgoing waves are related by the $M \times M$ scattering matrix $S(E)$. The

*jack.kuipers@bristol.ac.uk
†m.sieber@bristol.ac.uk

Wigner time delay, which represents the extra time spent in the scattering process compared to free motion, is defined as [20,21]

$$\tau_W(E) = -\frac{i\hbar}{M}\mathrm{Tr}\left[S^\dagger(E)\frac{dS(E)}{dE}\right] = -\frac{i\hbar}{M}\frac{d}{dE}\ln \det S(E). \quad (1)$$

The time delay can be expressed semiclassically both in terms of the trapped set of periodic orbits of the open system, and in terms of the open scattering trajectories that enter and exit through the leads.

The description of the Wigner time delay in terms of trapped periodic orbits comes from its relation to a density of states which, in general, is the difference between the level density of the open scattering system and a free system [22]

$$\tau_W(E) = \frac{2\pi\hbar}{M}d(E) \approx \frac{2\pi\hbar}{M}\bar{d}(E) + \frac{2\pi\hbar}{M}d^{\mathrm{fl}}(E). \quad (2)$$

Here the density of states $d(E)$ is separated into a mean part $\bar{d}(E)$ and a fluctuating part $d^{\mathrm{fl}}(E)$ which each have a semiclassical approximation. The approximation for the mean density of states, for a chaotic cavity with 2 degrees of freedom, comes from Weyl's law for the corresponding closed system $\bar{d}(E) \sim \Omega/(2\pi\hbar)^2$, where Ω is the phase space volume of the shell of constant energy E. The fluctuating part can be expressed, similar to the Gutzwiller trace formula [23], as a sum over the periodic orbits. The difference is that the sum only includes periodic orbits that are trapped in the system [24,14]. Using these approximations, we can write the time delay as

$$\tau_W(E) \approx \frac{T_H}{M} + \frac{2}{M}\mathrm{Re}\sum_{p,r} A_{p,r}(E)e^{i/\hbar r S_p(E)}e^{-i\pi/2 r\mu_p}, \quad (3)$$

where T_H is the Heisenberg time which is related to the average level density by $T_H = 2\pi\hbar\bar{d}(E)$. The first term is the average time spent in the cavity $\bar{\tau}_W = T_H/M$. It is equal to the inverse of the classical escape rate which can be expressed in the form $\mu = M/T_H$ [16]. In the sum p labels the trapped primitive periodic orbits and r their repetitions. The orbits have action S_p and Maslov index μ_p. Their stability amplitude $A_{p,r}$ can be written in terms of the stability matrix M_p and the period T_p

$$A_{p,r} = \frac{T_p}{\sqrt{|\det(M_p^r - 1)|}}. \quad (4)$$

The description of the time delay in terms of open trajectories comes from the semiclassical approximation to the scattering matrix elements [25,26,9]

$$S_{ba}(E) \approx \frac{1}{\sqrt{T_{\mathrm{H}}}}\sum_{\alpha(a\to b)} A_\alpha e^{i/\hbar S_\alpha}e^{-i\pi/2\nu_\alpha}. \quad (5)$$

Here S_α is the action of the trajectory α and ν_α is the number of conjugate points along the trajectory (plus twice the number of reflections on walls with Dirichlet boundary conditions). The stability amplitude A_α can be found in Ref. [26]. The sum is then over all classical trajectories that start in channel a and end in channel b, where the channels fix the absolute value of the angles at which the trajectories enter and leave the cavity. From this semiclassical approximation for the scattering matrix elements we can obtain an expression for the time delay by substituting into Eq. (1). When we differentiate the scattering matrix elements we ignore the change in the slowly varying prefactor and only keep the term from the oscillating action exponentials

$$\tau_W \approx \frac{1}{MT_H}\sum_{a,b}\sum_{\alpha,\alpha'(a\to b)} T_\alpha A_\alpha A_{\alpha'}^* e^{i/\hbar(S_\alpha - S_{\alpha'})}e^{-i\pi/2(\nu_\alpha - \nu_{\alpha'})}, \quad (6)$$

where $T_\alpha = \partial S_\alpha/\partial E$ is the time the trajectory α spends inside the system. Here we can see that the time delay is a sum over trajectory pairs α, α' both of which start and end in the same channels (a and b, respectively), followed by a sum over all the possible channels.

We can also consider a correlation function of scattering matrix elements

$$C(\epsilon) = \sum_{a,b} S_{ba}\left(E + \frac{\epsilon M}{4\pi\bar{d}}\right)S_{ba}^*\left(E - \frac{\epsilon M}{4\pi\bar{d}}\right), \quad (7)$$

where it is convenient to specify the energy difference in units of $M(2\pi\bar{d})^{-1} = \hbar\mu$, because this will simplify the formulas in the following. If we set $\epsilon = 0$ this becomes

$$C(0) = \mathrm{Tr}[S(E)S^\dagger(E)]. \quad (8)$$

By using the semiclassical approximation of the matrix elements from Eq. (5) and expanding the action up to first order in energy $S_\alpha(E+\eta) \approx S_\alpha(E) + \eta T_\alpha(E)$, the correlation function can be expressed in terms of pairs of scattering trajectories

$$C(\epsilon) \approx \frac{1}{T_H}\sum_{a,b}\sum_{\alpha,\alpha'(a\to b)} A_\alpha A_{\alpha'}^* e^{i/\hbar(S_\alpha - S_{\alpha'})} \times e^{-i\pi/2(\nu_\alpha - \nu_{\alpha'})}e^{i\epsilon\mu/2(T_\alpha + T_{\alpha'})}, \quad (9)$$

from which we can obtain a symmetrized version of the time delay [16]

$$\tau_W = \frac{-i}{\mu M}\frac{d}{d\epsilon}C(\epsilon)\Big|_{\epsilon=0} = -\frac{i\hbar}{2M}\mathrm{Tr}\left[S^\dagger(E)\frac{dS(E)}{dE} - S(E)\frac{dS^\dagger(E)}{dE}\right]. \quad (10)$$

Equation (10) agrees with the definition of the time delay in Eq. (1) because of the unitarity of the scattering matrix. If we insert Eq. (9) into Eq. (10) we obtain again a semiclassical formula for the time delay which differs slightly from Eq. (6) in that the time T_α is replaced by the average time $(T_\alpha + T_{\alpha'})/2$. Both formulas are equivalent and the difference only plays a role in Sec. V where it will be discussed. We use the relation of the time delay to the function $C(\epsilon)$ in the following to simplify the calculation by exploiting its similarity to the average conductance of a chaotic ballistic device [10,11]. In particular, we will obtain, as in the case of the conductance, simple diagrammatic rules for the semiclassical contributions of correlated trajectories.

Because we can express the time delay equally in terms of open trajectories and trapped periodic orbits, there should be a semiclassical equivalence between the two pictures and the following should hold:

$$\frac{1}{MT_H}\sum_{a,b}\sum_{\alpha,\alpha'(a\to b)} T_\alpha A_\alpha A^*_{\alpha'} \exp p^{i/\hbar(S_\alpha - S_{\alpha'})} e^{-i\pi/2(\nu_\alpha - \nu_{\alpha'})}$$

$$\approx \bar{\tau}_W + \frac{2}{M}\mathrm{Re}\sum_{p,r} A_{p,r}(E) e^{i/\hbar r S_p(E)} e^{-i\pi/2 r\mu_p}. \quad (11)$$

The left-hand side is the sum over scattering trajectories, while the right includes an average part and a sum over trapped periodic orbits. We shall now show how, by considering the contributions in the semiclassical limit of pairs of correlated trajectories from the sum on the left we can recreate all the terms on the right. We will consider only systems with two degrees of freedom, but the calculations are very similar in higher dimensions [6]. The assumptions for the semiclassical calculations in this article are the same as for the conductance in Ref. [11]. In particular, corrections related to the finite value of the quotient of the Ehrenfest time and the dwell time are neglected [27,28,12].

III. THE AVERAGE TIME DELAY

In this section we shall derive the average time delay from correlated pairs of open trajectories. For systems without time-reversal symmetry the diagonal approximation (pairing a trajectory with itself) suffices [16]. For systems with time-reversal symmetry, however, a small correction is needed which comes from trajectories that have close self-encounters. The calculation follows similar steps and ideas to the calculation of the average conductance [9–11], which in turn builds on work on spectral statistics [6]. We exploit this similarity by concentrating on the correlation function of the scattering matrix elements $C(\epsilon)$. Its semiclassical approximation is given by Eq. (9) which, aside from the exponential factor containing the trajectory time T_α and a different channel sum, is the same as the conductance from Ref. [11], so we only highlight the relevant points in the calculation. We shall be more detailed in Sec. IV where we introduce the new correlations that produce the periodic orbit terms.

The diagonal term for the sum over trajectories that connect channels a and b considers pairs where the two trajectories α and α' are identical, and it gives a contribution of

$$\frac{1}{T_H}\sum_{\alpha(a\to b)} |A_\alpha|^2 e^{i\epsilon\mu T_\alpha}. \quad (12)$$

The sum in Eq. (12) can be performed by using a sum rule for open trajectories [9] which turns it into an integral over the trajectory time T

$$\sum_{\alpha(a\to b)} |A_\alpha|^2 \cdots \approx \int_0^\infty dT\ e^{-\mu T}\cdots. \quad (13)$$

The exponential term in Eq. (13) represents the average probability that a trajectory remains in the system for the time T. The sum over channels depends on the symmetry of the dynamics. For systems without time-reversal symmetry ($\kappa=1$) we can pick both a and b from the M possible channels giving a factor of M^2. For systems with time-reversal symmetry ($\kappa=2$) we can also pair the trajectory α with its time reversal if the start and end channel are the same ($a=b$), and this contributes an additional M to the channel sum. The diagonal approximation thus becomes

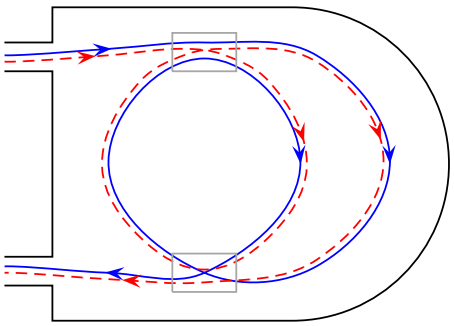

FIG. 1. (Color online) An example of a trajectory (full line) with two encounter regions and its partner trajectory (dashed line). The encounter regions are indicated by rectangular boxes.

$$C^{\mathrm{diag}}(\epsilon) \approx \frac{M(M+\kappa-1)}{T_H}\int_0^\infty dT\ e^{-\mu(1-i\epsilon)T} = \frac{M(M+\kappa-1)}{M(1-i\epsilon)}. \quad (14)$$

Using Eq. (10) this already leads to the correct result for the average time delay for systems without time reversal symmetry, but not for systems with time-reversal symmetry [because the prefactor then contains $M(M+1)$ instead of M^2]. Hence we need to consider off-diagonal contributions to the average of $C(\epsilon)$. They come from long trajectories that have one or more self-encounters in which two or more stretches of a trajectory are almost identical. In systems with time-reversal symmetry the stretches can also be almost mutually time reversed. The encounter regions are connected to each other and to the entry and exit channels by long parts of the trajectory called links. An example of a trajectory with two encounter regions is shown in Fig. 1. The partner trajectory connects the links in a different way in the encounter regions, but follows the original trajectory very closely along the links. Both encounter regions in the figure are examples of two-encounters which are traversed by two stretches of an orbit. In general an arbitrary number of $l\geq 2$ stretches of an orbit can be almost identical (up to time-reversal) in an encounter region and one then speaks of an l-encounter. The total numbers of the different encounter regions of a trajectory are collected in a vector $\boldsymbol{v}$ whose components v_l specify the numbers of l-encounters of a trajectory. For the calculation of the off-diagonal terms one has to consider all possible structures or families,[1] i.e., all topologically distinct ways in which two trajectories can be correlated. A more precise definition of families can be found in Ref. [11], but we shall

[1]The authors of Ref. [11] use the expression "structures" in the context of periodic orbits and "families" in the context of open trajectories.

need in the following only the fact that there is a sum rule for the number $N(\boldsymbol{v})$ of different families with the same vector $\boldsymbol{v}$. Further relevant quantities are the total number of encounters of a trajectory $V=\Sigma_l v_l$, and the total number of orbit stretches of a trajectory in the encounter regions $L=\Sigma_l l v_l$. The total number of links of a trajectory is then $L+1$.

The action difference of the trajectories is given in terms of coordinates along the stable and unstable manifolds in Poincaré surfaces of sections in the V encounter regions. These coordinates describe the relative positions of the different stretches of a trajectory. The encounter regions are labeled by σ and the number of trajectory stretches in them by l_σ. In the linearized approximation the action difference is given by

$$S_\alpha - S_{\alpha'} \approx \sum_{\sigma=1}^{V} \boldsymbol{s}_\sigma \cdot \boldsymbol{u}_\sigma = \boldsymbol{s} \cdot \boldsymbol{u}, \tag{15}$$

where $\boldsymbol{s}_\sigma$ and $\boldsymbol{u}_\sigma$ are vectors with dimension $(l_\sigma-1)$, and $\boldsymbol{s}$ and $\boldsymbol{u}$ contain the components of all these vectors.

The summation over the correlated trajectory pairs is simplified by the fact that different families with the same vector $\boldsymbol{v}$ give the same contribution [11]. Hence it is convenient to collect all these contributions and sum over all trajectories pairs whose correlations are specified by the vector $\boldsymbol{v}$. As for the diagonal approximation, we have also to take into account that one can pair a trajectory with the time-reverse of its partner orbit if $a=b$ in systems with time-reversal symmetry, and this gives an additional factor of two in these cases. This factor is denoted by η_{ab} in the following:

$$C^{\boldsymbol{v}}(\epsilon) \approx \frac{1}{T_H} \sum_{a,b} \eta_{ab} \sum_{\alpha,\alpha'(a\to b)}^{\text{fixed } \boldsymbol{v}} |A_\alpha|^2 e^{i/\hbar (S_\alpha - S_{\alpha'})} e^{i\epsilon \mu T_\alpha}, \tag{16}$$

where the approximations $T_\alpha \approx T_{\alpha'}$, $A_\alpha \approx A_{\alpha'}$, and $\mu_\alpha \approx \mu_{\alpha'}$ have been made, and

$$\eta_{ab} = 1 + (\kappa - 1)\delta_{ab}. \tag{17}$$

The sum over the trajectory pairs in Eq. (16) is performed by applying an ergodicity argument together with the finite escape probability of the scattering trajectories which results in replacing it by an integral

$$\sum_{\alpha,\alpha'(a\to b)}^{\text{fixed } \boldsymbol{v}} |A_\alpha|^2 \cdots \approx N(\boldsymbol{v}) \int dT \int d\boldsymbol{s}\, d\boldsymbol{u}\, w_{\boldsymbol{v},T}(\boldsymbol{s},\boldsymbol{u}) e^{-\mu T_{\text{exp}}} \cdots. \tag{18}$$

Here $N(\boldsymbol{v})$ is the number of families with the same vector $\boldsymbol{v}$, and T is the time of the trajectories. T_{exp} will be specified below, and $w_{\boldsymbol{v},T}(\boldsymbol{s},\boldsymbol{u})$ is the probability density that a trajectory of time T has self-encounters specified by the separation coordinates $\boldsymbol{s}$ and $\boldsymbol{u}$. It is given explicitly in terms of an integral over L of the $L+1$ link times

$$w_{\boldsymbol{v},T}(\boldsymbol{s},\boldsymbol{u}) = \int' dt_1 \cdots dt_L \frac{1}{\Omega^{L-V} \prod_{\sigma=1}^{V} t_{\text{enc}}^\sigma(\boldsymbol{s},\boldsymbol{u})}, \tag{19}$$

where t_i is the time of link i and t_{enc}^σ is the time of encounter in the encounter region σ. The prime at the integral denotes that it is subject to the restrictions that the link times must be positive. Furthermore, the total time of the links and encounter stretches is the time of the trajectory

$$T = \sum_{i=1}^{L+1} t_i + \sum_{\sigma=1}^{V} l_\sigma t_{\text{enc}}^\sigma, \tag{20}$$

and the time of the last link t_{L+1}, which is fixed by T and the L other link times, has to be positive too. The encounter times t_{enc}^σ are specified by requiring that all the components of $\boldsymbol{s}_\sigma$ and $\boldsymbol{u}_\sigma$ that determine the separation of the different stretches of a trajectory in the encounter region σ have a modulus that is smaller than a small arbitrary constant c, and it is given by

$$t_{\text{enc}}^\sigma \approx \frac{1}{\lambda} \ln \frac{c^2}{\max_i |s_{\sigma_i}| \times \max_j |u_{\sigma_j}|}, \tag{21}$$

where λ is the Lyapunov exponent. The relevant encounter times are of the order of the Ehrenfest time. Finally, the exposure time T_{exp} differs slightly from the time T of the trajectory, because the trajectory stretches during each encounter are very close together. If the trajectory survives during one crossing of the encounter region it will survive all the others crossings. The exposure time, the effective time where the trajectory can leave, is thus given by $T_{\text{exp}}=T-\Sigma_\sigma(l_\sigma-1)t_{\text{enc}}^\sigma$. Putting everything together, i.e., inserting Eqs. (18)–(20) into Eq. (16), one obtains after a change of the integration variable T to the last link time t_{L+1} an expression that contains integrals over all link times

$$C^{\boldsymbol{v}}(\epsilon) \approx \frac{N(\boldsymbol{v})}{T_H} \sum_{a,b} \eta_{ab} \prod_{i=1}^{L+1} \left(\int_0^\infty dt_i e^{-\mu(1-i\epsilon)t_i} \right) \times \prod_{\sigma=1}^{V} \left(\int d\boldsymbol{s}_\sigma d\boldsymbol{u}_\sigma \frac{e^{-\mu(1-i\epsilon l_\sigma)t_{\text{enc}}^\sigma} e^{i/\hbar \boldsymbol{s}_\sigma \cdot \boldsymbol{u}_\sigma}}{\Omega^{l_\sigma - 1} t_{\text{enc}}^\sigma} \right). \tag{22}$$

One can see that Eq. (22) factors into a product over the $L+1$ links and the V encounter regions. This is the main advantage of working with the correlation function $C(\epsilon)$ instead of directly with the time delay, because the corresponding expression for the time delay does not factorize [because of the T_α in the preexponential factor in Eq. (6)]. The factorization property will be useful also in the following sections. The integrals over coordinates in the encounter regions can be performed by using the semiclassical result [6,29]

$$\int d\boldsymbol{s}_\sigma d\boldsymbol{u}_\sigma (t_{\text{enc}}^\sigma)^k e^{i/\hbar a s_\sigma \boldsymbol{u}_\sigma} \approx \begin{cases} 0 & \text{if } k=-1, \\ \dfrac{1}{|a|} (2\pi\hbar)^{(l_\sigma - 1)} & \text{if } k=0, \end{cases} \tag{23}$$

where a is a real constant. (Strictly speaking, the result for $k=-1$ is a highly oscillatory term. This is an artifact of the sharp cutoff at c and can formally be removed by a small averaging.) The asymptotics of these integrals comes from the origin, or zero separation, at which point the semiclassical approximations made above become accurate. We can

now perform all the integrals in Eq. (22). The integral over the encounter regions is evaluated by expanding the exponential that contains the encounter times up to the linear term. Higher order terms in the expansion are neglected, because they are of the order of the quotient of the Ehrenfest time and the dwell time. For every encounter we obtain thus a contribution of $-\mu(1-i\epsilon l_\sigma)T_H^{l_\sigma-1}$, where $\mu=M/T_H$, and for every link a contribution of $\mu^{-1}(1-i\epsilon)^{-1}$. All the Heisenberg times cancel, and we obtain the simple diagrammatic rules that every link contributes a factor of $M^{-1}(1-i\epsilon)^{-1}$, and every encounter a factor of $-M(1-i\epsilon l_\sigma)$. Altogether the result is

$$C^{\boldsymbol{v}}(\epsilon) \approx N(\boldsymbol{v}) \sum_{a,b} \eta_{ab} \frac{(-1)^V \prod_{\sigma=1}^{V} (1-i\epsilon l_\sigma)}{M^{L-V+1}(1-i\epsilon)^{L+1}}. \tag{24}$$

As for the diagonal approximation the sum over the channels a and b gives a factor $M(M+\kappa-1)$. It is convenient to introduce $k=L-V+1$ and to combine the contributions from all vectors $\boldsymbol{v}$ with the same value of k. We can also include the diagonal term by saying it corresponds to a trajectory with no encounter $L=V=0$ and $N(\boldsymbol{v})=1$. With the diagonal term, all these trajectories give the average contribution to the correlation function

$$\bar{C}(\epsilon) \approx M(M+\kappa-1) \sum_{k=1}^{\infty} \sum_{\boldsymbol{v}}^{L-V+1=k} (-1)^V N(\boldsymbol{v}) \frac{\prod_{\sigma=1}^{V} (1-i\epsilon l_\sigma)}{M^k (1-i\epsilon)^{L+1}}. \tag{25}$$

We expand the result around $\epsilon=0$ and use $\Sigma_\sigma l_\sigma = L$ to obtain

$$\bar{C}(\epsilon) \approx M(M+\kappa-1) \sum_{k=1}^{\infty} \sum_{\boldsymbol{v}}^{L-V+1=k} \frac{(-1)^V N(\boldsymbol{v})}{M^k} [1+i\epsilon+O(\epsilon^2)]. \tag{26}$$

The sum over the vectors $\boldsymbol{v}$ can now be evaluated by using a sum rule for the numbers $N(\boldsymbol{v})$ that was obtained from a recursion relation in Ref. [11]

$$\sum_{\boldsymbol{v}}^{L-V+1=k} (-1)^V N(\boldsymbol{v}) = (1-\kappa)^{k-1}. \tag{27}$$

This leaves the evaluation of a geometric series to obtain

$$\bar{C}(\epsilon) \approx M[1+i\epsilon+O(\epsilon^2)], \tag{28}$$

which is the final result. Equation (28) shows first that the semiclassical approximation is consistent with the unitarity of the scattering matrix, because $\bar{C}(0)=\mathrm{Tr}\, S(E)S^\dagger(E) \approx M$. Second, one obtains the correct average time delay from the term that is linear in ϵ, $\bar{\tau}_W = T_H/M$.

IV. PERIODIC ORBIT TERMS

A. Periodic orbit encounters

The types of correlated trajectory pairs we will consider now approach a trapped unstable periodic orbit, follow it very closely, and leave it again. An example of such a trajectory is shown in Fig. 2. The trajectory approaches the periodic orbit almost along its stable manifold, goes around a number of times, and then leaves it closely following the unstable manifold. In the vicinity of the periodic orbit we describe the motion of the trajectory in a Poincaré surface of section transverse to the periodic orbit. Because of the Birkhoff-Moser theorem we can make a symplectic transformation to normal form coordinates which are along the stable and unstable manifolds. Close to a periodic orbit one can use the linearized approximation in which the Poincaré map has the simple form [30]

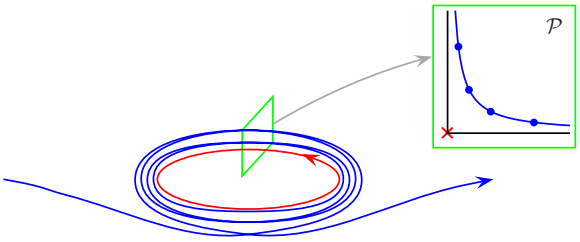

FIG. 2. (Color online) A schematic picture of a trajectory that approaches an unstable periodic orbit follows it a number of times and leaves it again. In a Poincaré map transverse to the periodic orbit the trajectory moves along the invariant hyperbola $su=$const.

$$s' = \Lambda_p^{-1} s, \quad u' = \Lambda_p u, \tag{29}$$

so that the trajectory moves along the invariant hyperbola $su=$const. Λ_p and $1/\Lambda_p$ are the eigenvalues of the stability matrix of the primitive periodic orbit p, with $|\Lambda_p|>1$. If Λ_p is negative the map involves also a reflection about the origin. The correlated trajectories that we will consider differ in the number of times they wind around the periodic orbit, and we shall see that the semiclassical periodic orbit contribution is obtained in the limit that su of these orbits goes to zero. This allows the application of the linearized approximation.

We have to specify how to count the number of times a trajectory winds around a periodic orbit. This can be done by fixing an arbitrary small positive constant c. The encounter region of the trajectory with the periodic orbit is then defined by requiring that the moduli of the coordinates s and u are both smaller than c. This is very similar to the definition of the self-encounter regions in the previous section. A very long trajectory has a finite probability to enter such an encounter region.

An example of a trajectory α which has $k=5$ intersections with the Poincaré surface in the encounter region $P_1,\ldots,P_5$ is shown in Fig. 3 (for positive Λ_p). Given such a trajectory one can find a partner trajectory with r more intersections in the encounter region in the following way. Consider the line through the first point P_1 that is formed by the intersections of trajectories that satisfy the required initial conditions for scattering trajectories (indicated by the thin line through P_1 in Fig. 3). There is second line through the last point P_k due to trajectories that satisfy the required final conditions (the thin line through P_5 in the figure). If one moves along the first line toward the stable manifold then one finds for every $r>0$ a unique point P_1' such that its $(k+r-1)$-th iterate by the Poincaré map P_{k+r}' lies on the second line. This is the

required partner trajectory α'. Figure 3 shows an example for $r=2$. In the following we will show that one obtains the semiclassical periodic orbit contributions from this kind of trajectory pairs. We first calculate the action difference of the trajectories. As a consequence of the Poincaré-Cartan theorem the action integral $\int \boldsymbol{p}d\boldsymbol{q}$ is independent of the path when it is evaluated on a surface that is formed by a continuous family of trajectories on the energy shell [30]. We apply this theorem to calculate three contributions to the action difference $\Delta S = S_\alpha - S_{\alpha'}$: $\Delta_i S$ coming from the initial parts of the trajectories up to P_1 and P_1', $\Delta_f S$ coming from the final parts of the trajectories from P_k and P_{k+r}' onwards, and $\Delta_m S$ from the remaining middle parts

$$\Delta_i S = \int_{P_1'}^{P_1} p dq, \quad \Delta_f S = \int_{P_k}^{P_{k+r}'} p dq,$$
$$\Delta_m S = \int_{P_1}^{O} p dq + \int_{O}^{P_k} p dq - \int_{P_1'}^{O} p dq$$
$$- \int_{O}^{P_{k+r}'} p dq - r S_p. \tag{30}$$

The first integral is evaluated along the line formed by trajectories with the required initial conditions (they are all exponentially close to each other at their starting points). The second integral is evaluated along the line formed by trajectories with the required final conditions (they are all exponentially close to each other at their end point). The remaining part of the action difference is obtained by comparing the actions of the middle parts of the trajectories to the action of the periodic orbit. The integrals are evaluated along lines that are formed by the intersection of trajectories that continuously connect the middle parts of the trajectories to, respectively, the k-fold and $(k+r)$-fold traversals of the primitive periodic orbit p. If we add up all contributions we obtain an integral over the two triangular regions $OP_1'P_1$ and OP_kP_{k+r} depicted in Fig. 3. The areas of these regions are invariant under the transformation to normal form coordinates. In the linearized approximation the sides of the triangles are straight lines. If $P_1=(u,s)$ then $P_1' \approx (u\Lambda_p^{-r}, s)$, $P_k \approx (u\Lambda_p^k, s\Lambda_p^{-k})$, $P_{k+r}' \approx (u\Lambda_p^k, s\Lambda_p^{-(k+r)})$, and one obtains [12]

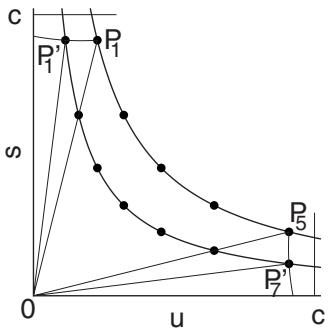

FIG. 3. Two trajectories which follow the periodic orbit at O five and seven times, respectively, within the region of the Poincaré section bounded by the constant c. The action difference is $S_\alpha - S_{\alpha'} = A - 2S_p$, where S_p is the action of the periodic orbit and A is the sum of the areas of the two triangles $OP_1'P_1$ and OP_5P_7'.

$$\Delta S = su(1 - \Lambda_p^{-r}) - rS_p. \tag{31}$$

We did the derivation for positive Λ_p, but the coordinates of the points and Eq. (31) hold also for negative Λ_p. In the case that Λ_p is negative and r is odd then P_1 and P_1' lie on different sides of the s-axis, and P_k and P_{k+r}' on different sides of the u axis.

Next we compare the semiclassical amplitudes of the trajectories α and α'. They depend on the stability matrices of the trajectories. The stability matrix describes the motion of neighboring trajectories in the linearized approximation. It gives the deviations at the final point of a trajectory in terms of the deviations at the initial point, in coordinates perpendicular to the trajectory

$$\begin{pmatrix} \delta q_f \\ \delta p_f \end{pmatrix} = M \begin{pmatrix} \delta q_i \\ \delta p_i \end{pmatrix}. \tag{32}$$

For cavities with leads the amplitude of a scattering trajectory is proportional to $|M_{21}|^{-1/2}$ where M_{21} is a matrix element of M [9]. The stability matrix can be composed by multiplying stability matrices for different parts of the trajectory. For the k iterations of the Poincaré map in the vicinity of the periodic orbit the stability matrix of α is approximated by the stability matrix of the periodic orbit p and hence we write $M_\alpha = M_f M_p^k M_i$ which i and f stand for the initial and final parts of the trajectory. The corresponding approximation for the trajectory α' is $M_{\alpha'} = M_f M_p^{k+r} M_i$. Powers of the two-dimensional stability matrix M_p can be written in terms of their eigenvalues as

$$M_p^k = \Lambda_p^k P_u + \Lambda_p^{-k} P_s \sim \Lambda_p^k P_u \quad \text{as} \quad k \to \infty, \tag{33}$$

where P_s and P_u are the projection operators onto the eigenvectors of M_p in the stable and unstable directions, respectively. As a consequence $M_{\alpha'} \sim M_\alpha \Lambda_p^r$ as $k \to \infty$, and we obtain the approximation

$$A_{\alpha'} \approx A_\alpha |\Lambda_p|^{-r/2}. \tag{34}$$

It is convenient to have the following geometrical picture. One considers a neighboring trajectory with initial infinitesimal deviation $\delta q_i \neq 0$ and $\delta p_i = 0$ and follows the development of this deviation in time as one moves along the trajectory. A conjugate point occurs every time the projection of the deviation onto the (orthogonal) p direction is zero, and the index ν increases by 1. (For billiard with Dirichlet boundary conditions it increases also by two for every reflection on the wall.) The matrix element M_{21} is equal to the projection at the final point. During the time the trajectory follows the periodic orbit, the deviation is aligned and stretched along the unstable direction, according to Eq. (33), and rotates with it around the periodic orbit. The Maslov index of the periodic orbit is the number of times the stable and unstable manifolds rotate by half a turn [31] (plus twice the number of reflections on walls with Dirichlet boundary conditions). After each traversal of the periodic orbit, the manifolds are back where they started and the Maslov index is an integer. As long as both α and α' are close to the periodic orbit, α' will pick up r times the Maslov index of the orbit p over the trajectory α. Outside of the encounter,

both trajectories are close to each other and have the same index, giving

$$\nu_{\alpha'} = \nu_\alpha + r\mu_p. \tag{35}$$

We mention that this geometrical picture can be generalized to systems with higher degrees of freedom $f>2$. Then one considers the development of an $(f-1)$-dimensional volume element in time that is formed at the initial point by infinitesimal deviations in the $(f-1)$ q-directions orthogonal to the trajectory.

We can now put the trajectory pairs that follow a trapped periodic orbit p in this way into the semiclassical sum for $C(\epsilon)$, Eq. (9). The times of the two trajectories are related by $T_{\alpha'} \approx T_\alpha + rT_p$. We insert furthermore Eqs. (31), (34), and (35) into Eq. (9) and take into account a factor of two if the channels a and b are the same in systems with time reversal symmetry, because then one can pair a trajectory also with the time-reverse of its partner. This factor is denoted as before by η_{ab}, see Eq. (17). We are left with the following to evaluate:

$$C^{p,r}(\epsilon) \approx \sum_{a,b} \eta_{ab} \frac{e^{-i/\hbar r S_p + i\pi/2 r\mu_p} e^{i\epsilon\mu/2rT_p}}{T_H |\Lambda_p|^{r/2}} \times \sum_{\alpha(a\to b)} |A_\alpha|^2 e^{i/\hbar su(1-\Lambda_p^{-r})} e^{i\epsilon\mu T_\alpha} + (r \to -r). \tag{36}$$

The last term denotes the same contribution with r replaced by $-r$. It is obtained from interchanging α and α' in the double sum over trajectories (9). The remaining step consists in performing the sum over all trajectories α that enter the encounter region of the periodic orbit p. This summation is performed by applying the ergodicity property that very long trajectories explore the available phase space volume uniformly, combined with the finite escape probability of the scattering trajectories. As a consequence the sum over trajectories, with the amplitudes as weight factors, are replaced by an integral (for related sum rules in closed systems see Ref. [32])

$$\sum_{\alpha(a\to b)} |A_\alpha|^2 \cdots \approx \int dT \int ds\, du w_{p,T}(s,u) e^{-\mu T_{\exp}} \cdots, \tag{37}$$

where T is the total time of the trajectory $(=T_\alpha)$ and $w_{p,T}$ is the probability density that a trajectory of time T goes through a surface element $dsdu$ around the point (u,s) in a fixed Poincaré section transverse to the periodic orbit p. The integrals over s and u are limited by the constant c. The time $T_{\exp}$ is the time during which the orbit can escape. It differs from the time T of the trajectory, because the trajectory cannot escape during the time it follows the trapped periodic orbit in the encounter region of the orbit (if one chooses the arbitrary constant c sufficiently small). Hence, the difference between T and $T_{\exp}$ is the time in the encounter region which is given by

$$t^p_{\text{enc}} \approx kT_p \approx \frac{1}{\lambda_p} \ln \frac{c^2}{|us|}, \tag{38}$$

where k is the number of iterations in the encounter region, and the Lyapunov exponent λ_p of the periodic orbit is obtained from $|\Lambda_p| = e^{\lambda_p T_p}$. The number k was obtained by using Eq. (29) from which follows that $k \approx \frac{1}{\lambda_p T_p} \ln \frac{c}{|u|} + \frac{1}{\lambda_p T_p} \ln \frac{c}{|s|}$. It is remarkable that Eq. (38) has the same form as the encounter time for self-encounters (21). For this reason, the central relation (23) for the integrals over s and u holds as well and will be used in the following.

The probability density $w_{p,T}(s,u)$ is obtained by noting that the probability that an element of a trajectory of time dt enters the surface element $ds\, du$ is given by

$$\frac{ds\, du\, dt}{\Omega}. \tag{39}$$

The probability density follows as

$$w_{p,T}(s,u) = \int_0^{T - t^p_{\text{enc}}} dt_1 \frac{T_p}{\Omega t^p_{\text{enc}}}, \tag{40}$$

where t_1 is the time at the intersection with the Poincaré surface. Equation (40) contains the factor $T_p/t^p_{\text{enc}} \approx 1/k$ to remove the multiple counting of a trajectory, because k points in the Poincaré section correspond to the same trajectory. We substitute Eqs. (37) and (40) into Eq. (36) and change the integration variable from T to t_2, where t_2 is the time from the encounter region to the exit channel, $T = t_1 + t^p_{\text{enc}} + t_2$, and obtain

$$C^{p,r}(\epsilon) \approx \sum_{a,b} \eta_{ab} \frac{T_p e^{-i/\hbar r S_p + i\pi/2 r\mu_p} e^{i\epsilon\mu/2rT_p}}{T_H |\Lambda_p|^{r/2}} \times \int ds\, du \frac{e^{i/\hbar su(1-\Lambda_p^{-r})} e^{i\epsilon\mu t^p_{\text{enc}}}}{\Omega t^p_{\text{enc}}} \prod_{i=1}^{2} \int_0^\infty dt_i \times e^{-\mu(1-i\epsilon)t_i} + (r \to -r). \tag{41}$$

We see again that the expression factorizes into contributions from the links and the encounter region. This implies that the diagrammatic rules can be extended, and that one gets additional contributions from the periodic orbit encounters. We can now perform the integral over s and u. Note that this integral automatically sums over trajectories α with an arbitrary number k of windings around the periodic orbit. We expand the integrand in ϵ up to first order and use Eq. (23). Only the term with t^p_{enc} in the numerator cancels with the encounter time in the denominator and contributes semiclassically. After integrating there is again a cancellation of Heisenberg times and the diagrammatic rule for the rth repetition of a periodic orbit p follows as

$$2i\epsilon\mu A_{p,r} \cos\left(-\frac{1}{\hbar} r S_p + \frac{\pi}{2} r\mu_p + \frac{\epsilon\mu}{2} r T_p \right), \tag{42}$$

where we used the identity $\sqrt{|\det(M_p^r - 1)|} = |\Lambda_p|^{r/2} |1 - \Lambda_p^{-r}|$. The semiclassical contribution (42) comes from all the trajectory pairs for which one trajectory winds r more times around the periodic orbit p than its partner. The contribution comes from the close vicinity of the origin, i.e., from trajectory pairs for which the total number of windings around the periodic orbit is very large. The diagrammatic rules that we

TABLE I. Diagrammatic rules for the different contributions to the correlation function $C(\epsilon)$.

contribution of each link	$\frac{1}{M(1-i\epsilon)}$
contribution of each l-encounter	$-M(1-il\epsilon)$
rth contribution of a periodic-orbit encounter	$2i\epsilon\mu A_{p,r}\cos(-\frac{1}{\hbar}rS_p+\frac{\pi}{2}r\mu_p+\frac{1}{2}\epsilon\mu rT_p)$
rth contribution of periodic-orbit plus l-encounter	$2il\epsilon\mu A_{p,r}\cos(-\frac{1}{\hbar}rS_p+\frac{\pi}{2}r\mu_p+\frac{1}{2}\epsilon\mu rT_p)$

have encountered so far are the first three in Table I, and the total contribution to $C(\epsilon)$ follows as

$$C^{p,r}(\epsilon)\approx\sum_{a,b}\eta_{ab}\frac{2i\epsilon\mu}{M^2(1-i\epsilon)^2}A_{p,r}\times\cos\left(-\frac{1}{\hbar}rS_p+\frac{\pi}{2}r\mu_p+\frac{\epsilon\mu}{2}rT_p\right). \quad (43)$$

Finally we perform the sum over the channels which gives a factor $M(M+\kappa-1)$ as in Sec. III. The result is

$$C^{p,r}(\epsilon)\approx 2i\epsilon\mu\frac{M(M+\kappa-1)}{M^2}A_{p,r}\times\cos\left(-\frac{1}{\hbar}rS_p+\frac{\pi}{2}r\mu_p\right)+O(\epsilon^2). \quad (44)$$

In the case of systems without time-reversal symmetry ($\kappa=1$) this yields exactly the contribution of the rth repetition of the trapped periodic orbit to the time delay. However, for systems with time-reversal symmetry the prefactor is slightly wrong. The reason for this is the same as why the diagonal approximation in Sec. III did not give the correct mean time delay. There are other correlations between trajectories that have to be included. So far we have considered trajectory pairs, α and α', which differ only in the number of windings around the periodic orbit p. However, the orbit α can also have additional close self-encounters. As a consequence, α and α' can differ also in the way in which different links are connected in the encounter regions of the self-encounters. We will see in the next section that this leads to a variety of further correlations.

B. Combinations of periodic orbit encounters and self-encounters

Consider a trajectory pair with self-encounters. The number and types of the self-encounters are specified by the vector $\boldsymbol{v}$. In addition, the trajectory pair can have an encounter with a periodic orbit. We consider first the situation where the periodic orbit encounter occurs during one of the $(L+1)$ links. The additional encounter divides a link into two parts and increases the total number of links to $(L+2)$. The joint probability density for this case is

$$w_{\boldsymbol{v},p,T}(\boldsymbol{s},\boldsymbol{u})=\int' dt_1\cdots dt_{L+1}\frac{T_p}{\Omega^{L+1-V}t_{\mathrm{enc}}^p\prod_{\sigma=1}^{V}t_{\mathrm{enc}}^{\sigma}}, \quad (45)$$

where the prime again denotes that all link times, including the remaining one t_{L+2}, have to be positive [see discussion around Eq. (20)]. With this probability density one finds again that the contribution to the correlation function $C(\epsilon)$ factorizes and that it can be obtained by the diagrammatic rules that have been derived in the previous sections. They are summarized in the first three lines of Table I. After a summation over the channels one obtains

$$C_1^{\boldsymbol{v},p,r}(\epsilon)\approx(L+1)\frac{M(M+\kappa-1)}{M^{L-V+2}}N(\boldsymbol{v})(-1)^V 2i\epsilon\mu A_{p,r}\times\cos\left(-\frac{1}{\hbar}rS_p+\frac{\pi}{2}r\mu_p\right)+O(\epsilon^2). \quad (46)$$

There is a factor $(L+1)$, because the periodic orbit encounter can occur during any of the original $(L+1)$ links.

One can also have the situation that a periodic orbit encounter overlaps with a self-encounter. In other words a self-encounter occurs in the vicinity of a periodic orbit. This leads to interesting consequences. In the simplest situation a two-encounter occurs in the vicinity of a periodic orbit in a system with time-reversal symmetry. A Poincaré section for this case is shown in Fig. 4. An orbit α, indicated by the full lines, has a first encounter with the periodic orbit, and its intersection points with the Poincaré section follow a hyperbola in the downward direction (the direction is indicated by arrows). Then the trajectory goes away from the periodic orbit, makes a loop and comes back and follows the periodic orbit in the opposite direction. The (time-reverses of) the intersection points with the Poincaré surface then follow a second hyperbola in the upward direction. (When we speak of the intersection points of α in the following, we mean this to include the intersection points of its time reverse.)

This situation is different from a usual two-encounter where α has only two intersection points with the Poincaré surface (u_1,s_1) and (u_2,s_2). In a usual two-encounter the partner orbit α' has intersection points which are approximately given by (u_1,s_2) and (u_2,s_1), i.e., they are obtained by drawing a rectangle with the intersection points of α in opposite corners. If we apply this picture to find the partner orbit in Fig. 4 we see that we have several possibilities to use this construction to find a partner orbit which traverses the loop in the opposite direction, because α has many intersection points. Some of these possibilities lead to the same partner trajectory. For example, in Fig. 4 the rectangles that are between the two full lines yield a partner trajectory that follows the two dashed hyperbolae that lie between the two full hyperbolae. If other intersection points of α are connected by rectangles, then other partner trajectories are obtained. Figure 4 shows one further example by the dashed hyperbolae that lie outside the full hyperbolae. However, there are more possibilities that are not shown in the figure. The number k of rectangles that correspond to the same partner trajectory

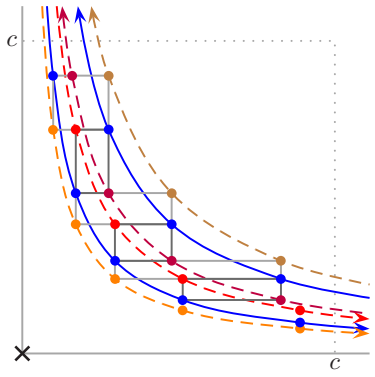

FIG. 4. (Color online) An example of a trajectory (the dots on the two full lines) with a two-encounter in the vicinity of a periodic orbit and some of its partner trajectories (the dots on the dashed lines). The partner trajectories are obtained by drawing rectangular boxes which have points of the original trajectory (full lines) in opposite corners.

follow from the Poincaré mapping (29) with $|\Lambda_p|=e^{\lambda_p T_p}$. It has the form $k=\frac{1}{\lambda_p T_p}\ln\frac{c}{\max_j|u_j|}+\frac{1}{\lambda_p T_p}\ln\frac{c}{\max_j|s_j|}$. This suggests the following definition of the encounter time:

$$t_{\rm enc}^{p,\sigma}\approx kT_p\approx\frac{1}{\lambda_p}\ln\frac{c^2}{\max_i|s_i|\times\max_j|u_j|}, \tag{47}$$

which has a close similarity to Eq. (21).

The occurrence of several partner orbits can be understood in the following way. A partner trajectory α' of α differs in the direction in which the loop between the two periodic orbit encounters is traversed. However, it can also differ in the number of times it follows the periodic orbit before and after the loop, as long as the total number of traversals is the same as for α. For example, if α has k_1 intersections in the square of the Poincaré section with side lengths c before the loop, and k_2 intersections after the loop, then the partner trajectory can have k_1+d intersections before the loop and k_2-d intersections after the loop, where d is any integer with $k_1+d>0$ and $k_2-d>0$. This means that the presence of the periodic orbit leads to a large number of possible partner trajectories.

However, we are interested in obtaining the periodic orbit contributions to the time delay. Hence we have to consider trajectories α'' which have altogether r more periodic traversals than the trajectories α'. These trajectories α'' then differ from the original trajectories α in the number of periodic orbit traversals as well as in the direction in which the loop is traversed. In the following we calculate the semiclassical contribution of the trajectory pairs α and α''.

Let us consider the general case that an l-encounter occurs near a periodic orbit p. A partner orbit α' is obtained by reconnecting the links in a different way in the encounter region. This reconnection is specified by a permutation $\pi(j)$, $j=1,\ldots,l$ which consists of one cycle of length l [6,29]. The action difference in [6,29] can be expressed in the form $\Delta S=\Sigma_{j=1}^{l}s_j(u_j-u_{\pi(j)})$. If we now consider partner trajectories α'' that have additional periodic orbit traversals $r_1,\ldots,r_l$ during the l encounters with the periodic orbit, with $\Sigma_j r_j=r$, then the action difference with α changes according to Eq. (31) and is given by

$$\Delta S=\sum_{j=1}^{l}s_j(u_j-u_{\pi(j)}\Lambda_p^{-r_j})-rS_p=\boldsymbol{s}^{\rm T}B\boldsymbol{u}-rS_p, \tag{48}$$

where $\boldsymbol{s}$ and $\boldsymbol{u}$ are the vectors of the l coordinates in the stable and unstable directions, and $B=I+\widetilde{B}$ where $\widetilde{B}_{ji}=-\delta_{i\pi(j)}\Lambda_p^{-r_j}$. We have $\det B=1+\det\widetilde{B}$, because the permutation consists of one cycle of length l. Furthermore, $(l-1)$ column exchanges bring $\widetilde{B}$ into diagonal form, and hence $\det\widetilde{B}=-\Lambda_p^r$ and $\det B=1-\Lambda_p^r$.

If we have one l-encounter σ in the vicinity of a periodic orbit p, and no further self-encounters, then the probability density is given by

$$w_{\sigma,p,T}(\boldsymbol{s},\boldsymbol{u})=\int' dt_1\cdots dt_l\frac{T_p}{\Omega^l t_{\rm enc}^{p,\sigma}}, \tag{49}$$

where the encounter time is given in Eq. (47). The factor $1/k=T_p/t_{\rm enc}^{p,\sigma}$ takes care of the overcounting of trajectory pairs. The contribution to $C(\epsilon)$ follows from Eqs. (36), (37), and (49) as

$$\sum_{a,b}\eta_{ab}\frac{T_p e^{-i/\hbar rS_p+i\pi/2r\mu_p}e^{i\epsilon\mu/2rT_p}}{T_H|\Lambda_p|^{r/2}}\times\int ds\,du\frac{e^{i/\hbar\boldsymbol{s}^T B\boldsymbol{u}}e^{il\epsilon\mu t_{\rm enc}^{p,\sigma}}}{\Omega^l t_{\rm enc}^{p,\sigma}}\times\prod_{i=1}^{l+1}\int_0^\infty dt_i e^{-\mu(1-i\epsilon)t_i}+(r\to-r). \tag{50}$$

The expression factorizes again, and the contribution from the encounter region is obtained by expanding the exponential which contains the encounter time. The contribution originates again from the linear term of this expansion. The resulting diagrammatic rule is listed in the forth line of Table I. Note that the contribution does not depend on how the repetition number r is split into parts $r_1,\ldots,r_l$. In fact, the integral over the $\boldsymbol{s}$ and $\boldsymbol{u}$ coordinates sums over the different ways of splitting r into parts, because a trajectory α has many intersection points. The different $\boldsymbol{s}$ and $\boldsymbol{u}$ coordinates for these intersection points correspond to different ways of splitting r, as in Fig. 4 and the discussion after Eq. (47).

Finally, we include the possibility that there are additional self-encounters which are not near a periodic orbit. One finds that also in this case the contributions factorize, and they can be evaluated by the rules in Table I. If the total number of self-encounters is given by the vector $\boldsymbol{v}$, and we sum over all the cases where one of the V self-encounters is in the vicinity of the periodic orbit p, we obtain

$$C_{\rm II}^{\boldsymbol{v},p,r}(\epsilon)\approx(-\sum_\sigma l_\sigma)\frac{M(M+\kappa-1)}{M^{L-V+2}}N(\boldsymbol{v})(-1)^V 2i\epsilon\mu A_{p,r}\times\cos\left(-\frac{1}{\hbar}rS_p+\frac{\pi}{2}r\mu_p\right)+O(\epsilon^2). \tag{51}$$

This expression differs from Eq. (46) in that the factor $(L+1)$ is replaced by $-\Sigma_\sigma l_\sigma = -L$. When we add the two this factor becomes 1. Finally we sum over all vectors $\boldsymbol{v}$ and include also the contributions from Sec. IV A [corresponding to $L=V=0$ and $N(\boldsymbol{v})=1$]

$$C^{p,r}(\epsilon) \approx (M+\kappa-1)\sum_{k=1}^{\infty}\sum_{\boldsymbol{v}}^{L-V+1=k}\frac{N(\boldsymbol{v})(-1)^V}{M^k}2i\epsilon\mu A_{p,r} \times\cos\left(-\frac{1}{\hbar}rS_p+\frac{\pi}{2}r\mu_p\right)+O(\epsilon^2)$$

$$\approx 2i\epsilon\mu A_{p,r}\cos\left(-\frac{1}{\hbar}rS_p+\frac{\pi}{2}r\mu_p\right)+O(\epsilon^2), \quad (52)$$

where the sum rule (27) for $N(\boldsymbol{v})$ has been used.

Equation (52) is the final result of this section. Using Eq. (10), it gives the correct contribution of the rth repetition of the periodic orbit p to the time delay (3) in systems with or without time reversal symmetry.

We have seen in this section that the vicinity of a periodic orbit gives rise to a rich variety of correlations between trajectories. We concentrated on those correlations that are responsible for the semiclassical periodic orbit terms of the time delay. There are further correlations which we do not explore in the present article. One example are the trajectory pairs of this section with $r=0$. There can also be multiple encounters with a periodic orbit p which do not correspond to the picture that one of the usual self-encounters occurs near a periodic orbit. An example is a trajectory which visits a periodic orbit twice and follows it both times in the same direction and has no further self-encounters. Furthermore, a trajectory can have encounters with several different periodic orbits. These terms, however, appear in higher order terms in the expansion in ϵ. (Visits of n periodic orbits appear in terms of order ϵ^n.) These additional correlations merit further study.

An interesting question is whether one obtains periodic orbit contributions to the conductance with the type of open orbit correlations in this section. The Landauer-Büttiker formulation for the conductance can be obtained, in certain situations, from linear response theory (Kubo formula). On the other hand, when the Kubo approach is applied to the bulk conductivity in antidot lattices it gives semiclassical expressions in terms of periodic orbits [26]. It is an open question whether periodic orbit contributions exist for the Landauer-Büttiker conductance as well.

The conductance is proportional to the total transmission through the cavity

$$\mathcal{T}=\sum_{b_{\rm out}a_{\rm in}} S_{b_{\rm out}a_{\rm in}}(E)S^*_{b_{\rm out}a_{\rm in}}(E), \quad (53)$$

where the only difference to $C(\epsilon)$ lies in the different channel sum (the sum is over incoming and outgoing channels), and $\epsilon=0$. Since the periodic orbit contributions to $C(\epsilon)$ in Eq. (52) vanish in the limit $\epsilon=0$ one finds that there is no periodic orbit contribution to the conductance as well in this leading order semiclassical calculation. This does not completely rule out the possibility of periodic orbit terms in the conductance, but if they exist they need to have a different sign in the reflectance, because transmission and reflectance have to add up to a constant, the number of channels in the incoming lead(s).

V. CORRELATION FUNCTIONS OF THE TIME DELAY

In this section we look at a correlation function of the time delay, and show that it is possible to get the leading order result of RMT using open trajectories. This addresses the concern of Ref. [16] that the diagonal approximation in the approach using trajectories gave a different result. The key is that there are other contributions of the same order as the diagonal approximation for open trajectories, and these need to be included to get the leading order term [18]. The calculation for the correlation function of the time delay is similar to that for the conductance variance and, in particular, to the Ericson fluctuations [11]. The correlation function that we consider is defined as

$$\tilde{R}_2(\omega,M)=\frac{\left\langle \tau_W\left(E+\frac{\omega M}{4\pi\bar{d}}\right)\tau_W\left(E-\frac{\omega M}{4\pi\bar{d}}\right)\right\rangle_E-\bar{\tau}_W^2}{\bar{\tau}_W^2}. \quad (54)$$

Again it is convenient to specify the energy difference in units of $M(2\pi\bar{d})^{-1}$. The correlation function involves an energy average over an energy range ΔE which is classically small, but encompasses many resonances $E\gg\Delta E\gg 1/\bar{d}(E)$. In RMT the leading order result for a large number of channels M is given for the two considered symmetry classes by [13,14]

$$\tilde{R}_2(\omega,M)=\frac{2\kappa}{M^2}\frac{1-\omega^2}{(1+\omega^2)^2}. \quad (55)$$

When we express the correlation function in Eq. (54) as a sum over quadruples of trajectories we subtract the term $\bar{\tau}_W^2$ by removing the trajectories pairs of Sec. III that give the mean delay time. Inserting the semiclassical approximation for the time delay (6) results in

$$\tilde{R}_2(\omega,M)=\frac{1}{T_H^4}\Big\langle\sum_{a,b}\sum_{c,d}{}'\sum_{\alpha,\alpha'(a\to b)}\sum_{\beta,\beta'(c\to d)} T_\alpha T_\beta A_\alpha A^*_{\alpha'}A_\beta A^*_{\beta'} \times e^{i/\hbar(S_\alpha-S_{\alpha'}+S_\beta-S_{\beta'})}e^{i\omega\mu/2(T_\alpha-T_{\alpha'}-T_\beta+T_{\beta'})}\Big\rangle_E. \quad (56)$$

Here, α,α' are trajectories from channel a to b and β,β' are trajectories from channel c to d and we sum over trajectories and channels. The prime at the second sum indicates that we have removed the orbits where $\alpha\approx\alpha'$ and $\beta\approx\beta'$.

We start with the calculation of the diagonal contribution from Ref. [16]. Because we have removed the trajectory pairs that give the average time delay, we have to consider only the cases when $S_\alpha=S_{\beta'}$ and $S_\beta=S_{\alpha'}$. Without time reversal symmetry this means that $\alpha=\beta'$ and $\beta=\alpha'$, which requires that the channels $a=c$ and $b=d$. Hence we get a factor M^2 from the sum over the channels. With time reversal symmetry there are three additional cases. We can also have $\alpha=\bar{\beta}'$ and $\beta=\bar{\alpha}'$, where the overbar indicates the time re-

verse. This requires $a=d$ and $b=c$ and the channel sum gives M^2. Furthermore, we can have $\alpha=\beta'$ and $\beta=\bar{\alpha}'$, or $\alpha=\bar{\beta}'$ and $\beta=\alpha'$. Both cases require $a=b=c=d$ and each channel sum yields M. The total channel factor for the systems with time reversal symmetry is thus $2M(M+1)$, and in leading order for large M the channel factor for the two symmetry cases is $\sim\kappa M^2$. We can perform now the sums over the trajectory pairs by replacing them by an integral according to Eq. (13), and we perform the sum over the channels by multiplying with the channel factor

$$\tilde{R}_2^{\mathrm{diag}}(\omega,M) \approx \frac{\kappa M^2}{T_H^4}\int_0^\infty\int_0^\infty dT_\alpha dT_\beta T_\alpha T_\beta e^{-\mu(T_\alpha+T_\beta)}e^{i\omega\mu(T_\alpha-T_\beta)}, \tag{57}$$

which, after integrating, is

$$\tilde{R}_2^{\mathrm{diag}}(\omega,M) \approx \frac{\kappa}{M^2}\frac{1}{(1+\omega^2)^2}. \tag{58}$$

We have a factor of two different from the expected result (55), and a different functional form. To correct for this we have to add sums over quadruplets with encounters that contribute at the same order of M^{-1}. The reason why they can contribute at the same order as the diagonal term is because they have larger channel factors.

One example is a quadruplet where the trajectories α and β have one close encounter. Then their partner trajectories follow one of these two trajectories from the entrance channel to the encounter region where they switch over to the other trajectory and follow it to the exit channel, see Fig. 5 [or Fig. 4(j) in Ref. [11]]. If we label the link time betweens entrance or exit channels and the encounter region by t_i, then the times along α and β can be written as

$$T_\alpha = t_1 + t_{\mathrm{enc}} + t_2, \quad T_\beta = t_3 + t_{\mathrm{enc}} + t_4. \tag{59}$$

If α' follows first α and then β, and β' does vice versa, we have

$$T_{\alpha'} = t_1 + t_{\mathrm{enc}} + t_4, \quad T_{\beta'} = t_3 + t_{\mathrm{enc}} + t_2. \tag{60}$$

These quadruplets are only possible if channels b and d are identical. We can also interchange the role of α' and β' which requires that $a=c$. In systems with time reversal symmetry we have to consider also cases where the role of α' and/or β' is taken over by its time reverse, similar to the diagonal approximation. The sum over trajectories for these different configurations always gives the same result, hence it is sufficient to do the calculation for the case (60) and to perform the channel sum by multiplying with the total channel factor. In systems without time reversal symmetry this channel factor is $2M^3$, and in system with time reversal symmetry it is $4M^3+8M^2+4M$. In leading order it is hence $\sim 2\kappa M^3$.

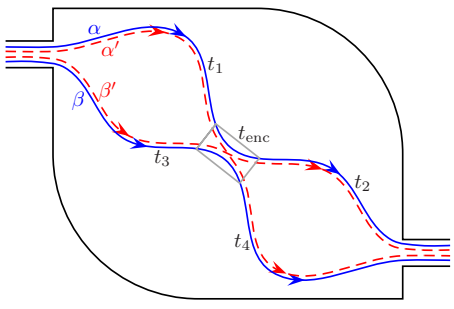

FIG. 5. (Color online) An example of a trajectory quadruplet where the trajectories α and β (full lines) have one two-encounter. Their partner trajectories (dashed lines) cross the encounter region differently. The encounter region is indicated by a rectangular box.

The difference in times for the case (60) is

$$\frac{1}{2}(T_\alpha - T_{\alpha'} - T_\beta - T_{\beta'}) = t_2 - t_4, \tag{61}$$

and the contribution to the correlation function is given by

$$\frac{2\kappa M^3}{T_H^4}\int_0^\infty dt_1 dt_2 dt_3 dt_4 e^{-\mu(t_1+t_2+t_3+t_4)}e^{i\omega\mu(t_2-t_4)} \times \int dsdu(t_1+t_{\mathrm{enc}}+t_2)(t_3+t_{\mathrm{enc}}+t_4)\frac{e^{-\mu t_{\mathrm{enc}}}}{\Omega t_{\mathrm{enc}}}e^{i/\hbar su}. \tag{62}$$

This then can be evaluated with the rule (23) and yields

$$\frac{2\kappa}{M^2}\frac{\omega^2}{(1+\omega^2)^2}. \tag{63}$$

Following a similar process we find the contribution from the other diagrams in Fig. 4 of Ref. [11] and give the results in Table II. When we now multiply these contributions by their channel factor $M^4+M^2\sim M^4$ for the unitary case and add the terms calculated above, we get the following result:

$$\frac{2}{M^2}\frac{1-\omega^2}{(1+\omega^2)^2}, \tag{64}$$

which is indeed the leading order term of Eq. (55). For the orthogonal case, the channel factor for the configurations in Table II is $M^4+2M^3+3M^2+2M\sim M^4$ to leading order. However there are additional trajectory quadruplets that contribute [Figs. 4(f)–4(h)] which are related to the quadruplets in Figs. 4(c)–4(e) by time reversal of parts of the structure. In fact these additional quadruplets just give the same contribution again as those in Figs. 4(c)–4(e). Therefore, the leading order contribution is simply twice that for the unitary case, again in line with Eq. (55).

It is worth noting here that using the symmetrized version of the time delay, Eq. (10) with Eq. (9), we get a different result for each trajectory quadruplet, but the sum of their contributions gives the same result as here. To calculate higher order terms, using the methods of Ref. [11], the similarities can be exploited by defining a "symmetrized" correlation function which can be written in terms of the correlation function of the scattering matrix elements

$$\tilde{R}_2(\omega,M) = \frac{-1}{M^2}\frac{d^2}{d\epsilon_1 d\epsilon_2}\left\langle C^{\mathrm{fl}}\left(\epsilon_1, E+\frac{\omega M}{4\pi\bar{d}}\right) \times C^{\mathrm{fl}}\left(\epsilon_2, E-\frac{\omega M}{4\pi\bar{d}}\right)\right\rangle_E\Bigg|_{\epsilon_1=\epsilon_2=0}, \tag{65}$$

where $C^{\mathrm{fl}}(\epsilon,E)$ is the semiclassical approximation to the fluctuating part of the correlation function of the scattering matrix elements at energy E. This means that the trajectory pairs responsible for the average part are removed. The calculation is very similar to that of the Ericson fluctuations. A complication in comparison to the calculation of the mean time delay in Sec. III is that one does not have one simple diagrammatic rule for every link. Each link is traversed by two of the four trajectories α, α', β, β', and the diagrammatic rule depends on which two of the four trajectories that are. The summation over the contributions from the different families is best done by a computer.

A final point is that if we consider $C^{\mathrm{fl}}(0,E)C^{\mathrm{fl}}(0,E)$ we are calculating

$$\{\mathrm{Tr}[S(E)S^{\dagger}(E)]-M\}^2 \tag{66}$$

which should be zero because of the unitarity of the scattering matrix. We checked this by using the formulas for the conductance variance [11], but with the appropriate channel factors that are given in this section. The result is indeed 0, and the unitarity of the scattering matrix is preserved by the semiclassical approximation if all semiclassical contributions are included.

VI. CONCLUSIONS

The time delay is an interesting quantity to study because of the two alternative semiclassical descriptions of it. The picture in terms of scattering trajectories is similar to the conductance, and by using the semiclassical methods of Ref. [11] which includes trajectories with self-encounters we obtained the average time delay. We considered also a correlation function of the time delay. Here the diagonal approximation is not enough to obtain the leading order term (as noted by Ref. [16]), because more complicated trajectory quadruplets with encounters contribute at the same order. By including these contributions we find that the unitarity of the semiclassical scattering matrix is restored, and that the semiclassical method does indeed provide an accurate description in agreement with RMT. This is as expected from other correlation functions in Ref. [11].

The main result of this article, however, is the evaluation of scattering trajectory correlations that recreate the periodic orbit terms of the time delay. These trajectories approach a periodic orbit, follow it closely some number of times, and then part from it. Approaching the orbit guarantees that they remain in the system, as long as the periodic orbit does and they remain close to it. This is the reason why only the trapped periodic orbits appear in the orbit sum of the time delay. For systems without time-reversal symmetry these periodic orbit encounters are enough to recreate the periodic orbit terms of the time delay, but for systems with time-reversal symmetry a small additional contribution is needed. We obtained this contribution from combinations of self-encounters and periodic orbit encounters.

TABLE II. Contribution of different types of trajectory quadruplets to the time delay correlation function. The labeling corresponds to Fig. 4 in Ref. [11].

4c	4d	4e
$\frac{-1-2\omega^2}{M^6(1+\omega^2)^2}$	$\frac{8\omega^2(1+\omega^2)}{M^6(1+\omega^2)^2}$	$\frac{2-2\omega^2-8\omega^2(1+\omega^2)}{M^6(1+\omega^2)^2}$

We found that the occurrence of self-encounters in the close vicinity of a periodic orbit leads to a wealth of new possible correlations between trajectories. We considered in this article only those correlations that are needed for the periodic orbit terms of the time delay, but there are further possible correlations. These new types of correlations deserve further study, and it can be expected that they play a role also in other contexts. For example, they might be relevant for periodic orbit correlations in closed systems, as envisioned in Ref. [33]. For the particular case of the Landauer-Büttiker conductance, however, we found that the trajectory correlations that yield the periodic orbit terms for the time delay do not give similar periodic orbit terms for the conductance.

ACKNOWLEDGMENTS

The authors would like to thank Eugene Bogomolny, Jon Keating, Sebastian Müller, Alfredo Ozorio de Almeida, and Raul Vallejos for helpful discussions and EPSRC for financial support. M.S. wishes to thank the Centro Brasileiro de Pesquisas Físicas for the kind hospitality during a sabbatical leave during which a major part of this research was carried out.

[1] O. Bohigas, M. J. Giannoni, and C. Schmit, Phys. Rev. Lett. **52**, 1 (1984).
[2] F. Haake, *Quantum Signatures of Chaos*, 2nd ed. (Springer, Berlin, 2001).
[3] J. H. Hannay and A. M. Ozorio de Almeida, J. Phys. A **17**, 3429 (1984).
[4] M. V. Berry, Proc. R. Soc. London, Ser. A **400**, 229 (1985).
[5] M. Sieber and K. Richter, Phys. Scr. **T90**, 128 (2001); M. Sieber, J. Phys. A **35**, L613 (2002).
[6] S. Müller, S. Heusler, P. Braun, F. Haake, and A. Altland, Phys. Rev. Lett. **93**, 014103 (2004); S. Müller, S. Heusler, P. Braun, F. Haake, and A. Altland, Phys. Rev. E **72**, 046207 (2005).
[7] S. Heusler, S. Müller, A. Altland, P. Braun, and F. Haake, Phys. Rev. Lett. **98**, 044103 (2007).
[8] J. P. Keating and S. Müller, Proc. R. Soc. London, Ser.A **463**, 3241 (2007).
[9] K. Richter and M. Sieber, Phys. Rev. Lett. **89**, 206801 (2002).
[10] S. Heusler, S. Müller, P. Braun, and F. Haake, Phys. Rev. Lett. **96**, 066804 (2006).

[11] S. Müller, S. Heusler, P. Braun, and F. Haake, New J. Phys. **9**, 12 (2007).
[12] P. W. Brouwer and S. Rahav, Phys. Rev. B **74**, 075322 (2006).
[13] B. Eckhardt, Chaos **3**, 613 (1993).
[14] R. O. Vallejos, A. M. Ozorio de Almeida, and C. H. Lewenkopf, J. Phys. A **31**, 4885 (1998).
[15] J. Kuipers and M. Sieber, Nonlinearity **20**, 909 (2007).
[16] C. H. Lewenkopf and R. O. Vallejos, J. Phys. A **37**, 131 (2004).
[17] R. O. Vallejos and C. H. Lewenkopf, J. Phys. A **34**, 2713 (2001).
[18] P. W. Brouwer, Phys. Rev. B **76**, 165313 (2007).
[19] P. Braun, S. Heusler, S. Müller, and F. Haake, J. Phys. A **39**, L159 (2006).
[20] E. P. Wigner, Phys. Rev. **98**, 145 (1955).
[21] F. T. Smith, Phys. Rev. **118**, 349 (1960).
[22] J. Friedel, Philos. Mag. **43**, 153 (1952).
[23] M. C. Gutzwiller, J. Math. Phys. **12**, 343 (1971).
[24] R. Balian and C. Bloch, Ann. Phys. **85**, 514 (1974).
[25] W. H. Miller, Adv. Chem. Phys. **30**, 77 (1975).
[26] K. Richter, *Semiclassical Theory of Mesoscopic Quantum Systems* (Springer, Berlin, 2000).
[27] S. Rahav and P. W. Brouwer, Phys. Rev. Lett. **96**, 196804 (2006).
[28] R. S. Whitney and P. Jacquod, Phys. Rev. Lett. **96**, 206804 (2006).
[29] S. Müller, Ph.D. thesis, Universität Duisberg-Essen, 2005.
[30] A. M. Ozorio de Almeida, *Hamiltonian Systems: Chaos and Quantization* (Cambridge University Press, Cambridge, 1988).
[31] S. C. Creagh, J. M. Robbins, and R. G. Littlejohn, Phys. Rev. A **42**, 1907 (1990).
[32] M. Sieber, J. Phys. A **32**, 7679 (1999).
[33] A. M. Ozorio de Almeida, Nonlinearity **2**, 519 (1989).